Received: 18 December 2020 | Revised: 9 February 2021 | Accepted: 28 February 2021

DOI: 10.1111/ppl.13383

BIOCHEMISTRY AND METABOLISM

Physiologia Plantarum

Visible light regulates anthocyanin synthesis via malate dehydrogenases and the ethylene signaling pathway in plum (*Prunus salicina* L.)

Guojing Zhang | Xiaohui Cui | Junping Niu | Fengwang Ma | Pengmin Li

State Key Laboratory of Crop Stress Biology for Arid Areas, College of Horticulture, Northwest A&F University, Yangling, China

Correspondence
Pengmin Li, State Key Laboratory of Crop Stress Biology for Arid Areas, College of Horticulture, Northwest A&F University, Yangling, Shaanxi 712100, China.
Email: lipm@nwsuaf.edu.cn

Funding information
National Natural Science Foundation of China, Grant/Award Number: 31972366

Edited by A. Krieger-Liszkay

Abstract

Light regulates anthocyanins synthesis in plants. Upon exposure to visible light, the inhibition of photosynthetic electron transfer significantly lowered the contents of anthocyanins and the expression levels of key genes involved in anthocyanins synthesis in plum fruit peel. Meanwhile, the expression levels of *PsmMDH2* (encoding the malate dehydrogenase in mitochondria) and *PschMDH* (encoding the malate dehydrogenase in chloroplasts) decreased significantly. The contents of anthocyanins and the levels of the key genes involved in anthocyanin synthesis decreased significantly with the treatment of 1-MCP (an inhibitor of ethylene perception) but were enhanced by the exogenous application of ethylene. The ethylene treatment could also recover the anthocyanin synthesis capacity lowered by the photosynthetic electron transfer inhibition. Silencing *PsmMDH2* and *PschMDH* significantly lowered the contents of anthocyanins in plum fruit. At low temperature, visible light irradiation induced anthocyanin accumulation in Arabidopsis leaves. However, the *mmdh*, *chmdh*, and *etr1-1* mutants had significantly lower anthocyanins content and expressions of the key genes involved in anthocyanins synthesis compared to wild type. Overall, the present study demonstrates that both photosynthesis and respiration were involved in the regulation of anthocyanin synthesis in visible light. The visible light regulates anthocyanin synthesis by controlling the malate metabolism via *MDH*s and the ethylene signaling pathway.

1 | INTRODUCTION

Anthocyanins are a group of water-soluble flavonoids and exist in various tissues of plants and make them appear red, blue, and purple colors. Anthocyanins can attenuate light to protect plants from photoinhibition/photodamage (Li et al., 2010; Smillie & Hetherington, 1999; Steyn et al., 2002). They also show strong antioxidant activity that might benefit plants and humans when consumed (Bi et al., 2014; Li et al., 2017; Nakabayashi et al., 2014; Neill et al., 2003). Besides, anthocyanin-rich foods can reduce starch consumption and delay glucose absorption, as anthocyanin may inhibit alpha-amylase and alpha-glucosidase (Xiao & Hogger, 2015).

The synthesis of anthocyanins in plants is most significantly regulated by light. The regulation mechanism of ultraviolet (UV) light on anthocyanins synthesis had been well documented in previous studies. These studies reported that UV light regulates the synthesis of anthocyanins through different photoreceptors, including the UV-B receptor UV RESISTANCE LOCUS 8 (UVR8) (Brosché & Strid, 2003; Brown et al., 2005; Christie et al., 2012) and the UV-A receptors phototropins (PHOTs) and cryptochrome 1 (CRY1) and CRY2 (Ahmad & Cashmore, 1993; Butler et al., 1959; Lin, 2000; Winslow & John, 2002). The two main domains of UVR8, the β-propeller domain and the C-terminal C27 domain, as well as the valine–proline (VP) motif of the CRY1 and CRY2 proteins, can bind CONSTITUTIVE

PHOTOMORPHOGENIC1 (COP1), and regulate the downstream transcription factors such as ELONGATED HYPOCOTYL5 (HY5), PRODUCTION OF ANTHOCYANIN PIGMENT 1 (PAP1) and PAP2 proteins (Maier et al., 2013; Ponnu et al., 2019; Yin et al., 2015). In apple, Li et al. (2012) reported that MdCOP1 negatively regulated the peel coloration by modulating the degradation of the MdMYB1 protein. Besides via the UV receptors, anthocyanin synthesis in apple peel could be regulated by the reactive oxygen species (ROS) produced by the plasma membrane NADPH oxidase under UV light (Chen et al., 2019; Zhang et al., 2015).

The anthocyanin synthesis in plants could also be regulated by visible light or be light independent. For instance, the roots of some potatoes (Liu et al., 2016; Vincenzo et al., 2014), sweet potatoes (Mano et al., 2007; Zhang et al., 2020), and carrots (Xu et al., 2019), the flesh of some apples (Chagné et al., 2013; Espley et al., 2007), kiwifruits (Wang et al., 2019), and plums (Niu et al., 2017) can accumulate abundant amounts of anthocyanins via the regulation of MYB transcription factors during their growth underground, or above the ground in the dark. After photosynthesis was interrupted, the anthocyanin synthesis was inhibited in turnip (Schneider & Stimson, 1971), corn (Kim et al., 2006), and Arabidopsis (Jeong et al., 2010). Under dark conditions, the aerobic respiration played an important role in anthocyanin synthesis in plum fruit by regulating the production of ATP and ethylene (Niu et al., 2017). The effect of ethylene on MYB transcription factors and anthocyanin synthesis has been widely reported in Arabidopsis (Lei et al., 2011), grape (El-Kereamy et al., 2003), and apple (An et al., 2018; Hu et al., 2019). It seems that ethylene is also involved in regulating anthocyanin synthesis in visible light. Using *ethylene response 1 (etr1-1)*, *ethylene insensitive 2 (ein2-1)*, and *ein3 ein3-like1* double mutants, Jeong et al. (2010) found that ethylene inhibited the expression of *sucrose transporter 1* (*SUC1*) and blocked the transport of sugar, leading to the interruption of photosynthesis and sugar promotion of anthocyanin synthesis. However, how visible light affects the production of ethylene is unknown.

It was reported that the accumulation of anthocyanin usually is accompanied by an increase in malate in vacuoles (Hu et al., 2016; Tohge et al., 2015). Malate is not only an important intermediate in the tricarboxylic acid cycle in respiratory metabolism but also participates in redox reactions in the chloroplasts. Malate works as an important substance for signal transmission among chloroplasts, cytoplasm, mitochondria, and other organelles (Noguchi & Yoshida, 2008; Shameer et al., 2019). For instance, the malate-oxaloacetate shuttle can transport the reducing power NADPH produced in chloroplasts to the cytoplasm in the form of malate, and the malate in the cytoplasm can be transported into mitochondria to participate in the respiratory metabolism (Noguchi & Yoshida, 2008; Shameer et al., 2019). We speculate that in visible light, photosynthesis might regulate the synthesis of anthocyanin through malate metabolism.

In this study, using plum fruits and the *malate dehydrogenase* (*mdh*) mutants of Arabidopsis, we investigated the relationship between malate metabolism and anthocyanin synthesis in visible light, to further explore the regulating mechanism of anthocyanin synthesis.

2 | MATERIALS AND METHODS

2.1 | Plant materials

The fruits of *Prunus salicina* "Red Beauty" was used in this study. The trees were 5-year-old on *Prunus persica* rootstock and planted with a spacing of 2×4 m in north–south rows in Yangling (34.29°N, 108.07°E; elevation: 500 m), Shaanxi province, China. They were approximately 2.5 m with a central leader. Nutrients, disease, and pest control were performed according to horticultural standards. Full bloom stage was at the end of March. The plum fruits were harvested at the veraison stage in June, with the fresh weight being around 37 ± 2 g per fruit.

Arabidopsis mutant *etr1-1* was donated by Dr. Hongwei Guo (Southern University of Science and Technology). SALK_087274C (*mmdh1*), SALK_016106C (*mmdh2*), SALK_102416 (*chmdh*), SALK_054146 (*cymdh1*), and SALK_097015 (*cymdh2*) were purchased from the Arabidopsis Biological Resource Center. After detection by amplifying the specific fragments on the T-DNA region (primers were listed on Table S1), the seeds of homozygotes were collected and stored at 4°C for subsequent experiments. Before planting, the seeds were soaked into 75% ethanol for 30 s, into 2.5% NaClO for 8 min, washed with sterile water 6 times, and then germinated on Murashige and Skoog (MS) medium agar plates (2.21 g L^{-1} MS salts, 10 g L^{-1} sucrose, and 7.5 g L^{-1} agar, pH 5.7) after disinfection. Seedlings were transplanted to soil 2 weeks after germination. Plants were grown in a light incubator with long-day photoperiods (16/8 h, light/dark) at 21°C for 30 days.

2.2 | Visible light treatments

Plum fruits were put into a light incubator (RXZ-430D, Dongnan Instruments Company), with the light intensity being 500 μmol m^{-2} s^{-1} provided by LED lights (The spectrum was shown in Figure S1). During treatment, the temperature in the incubator was set at 25°C and the relative humidity was 95%. Samples were taken before treatment (day 0) and after 2, 4, and 6 days of irradiation. For the chilling treatment of Arabidopsis, the same incubator was used with the temperature being set at 5°C for 10 days. For each genotype, 10 seedlings were used.

2.3 | Chemical treatments

For 3-(3′,4′-dichlorophenyl)-1,1-dimethylurea (DCMU), methyl viologen (MV), and ethephon treatments, the fruits were immersed into 20 μM DCMU, 20 μM MV, or 3 mM ethephon solution overnight. For 1-methylcyclopropene (1-MCP, an inhibitor of ethylene perception) treatment, fruits were put into a polyethylene plastic bag overnight, with a 1-MCP concentration of 1 μL L^{-1}. Parts of the fruits treated with 1-MCP were also immersed into 20 μM DCMU overnight, for the combined DCMU and ethephon treatment. Fruits

immersed in the solution without the chemicals were set as control. After 6 days of treatments, the peels were sampled with a peeler. All treatments were performed with five replicates. For each replicate, 10 fruits were used. The samples were immediately put into liquid nitrogen to freeze. After crushed in liquid nitrogen with a grinder from IKA® Works (VWR), the samples were stored at −80°C for subsequent assays.

2.4 | Phenolic compound analysis

Phenolic compounds in plum fruits or Arabidopsis leaves were extracted as described by Li et al. (2013) with some modifications. Briefly, for plum fruits, 0.5 g of samples were extracted with 1.6 ml of extract solution, containing 70% methanol and 2% formic acid. Whereas for Arabidopsis leaves, 0.15 g leaves were extracted with 1.8 ml of the extract solution. After centrifuging at 12000*g* for 15 min at 4°C, the supernatant of the plum samples was filtered with 0.22 μm filters before HPLC (LC20A, Shimadzu, Japan) assay as described by Li et al. (2013). The anthocyanin compounds were identified and quantified with authentic standards. For the assay of anthocyanin in Arabidopsis leaves, the supernatant was assayed at 520 nm with a spectrophotometer (UV 2450, Shimadzu).

2.5 | Nucleotide sugar, malate, and nicotinamide adenine dinucleotide (phosphate) analysis

The extraction and analysis of ATP and ADP were carried out as described by Li et al. (2014) with minor modifications. Briefly, 0.5 g for plum and 0.1 g for Arabidopsis frozen tissues were extracted with 1.2 ml of 6% $HClO_4$ and 5% insoluble polyvinylpolypyrrolidone at 0–4°C. After centrifugation at 12 000*g* for 10 min, 1 ml of the supernatant was neutralized with 90 μL of 5 M K_2CO_3. The supernatant was used to measure the metabolites using the HPLC (LC20A, Shimadzu, Japan). The supernatant was also used for malate analysis according to the method of Möllering (1974) with the spectrophotometer (UV 2450, Shimadzu). One milliliter reaction mixture contained 50 mM 3-amino-1-propanol-HCl (pH 10.0), 30 mM glutamate-NaOH (pH 10.0), 2.7 mM NAD^+, 1 unit glutamate-oxaloacetate transaminase, 10 units malate dehydrogenase (MDH), and 5 μL extract. Before and after adding the MDH, the absorbance at 340 nm was recorded.

The extraction of NADPH, $NADP^+$, NADH, and NAD^+ was performed as described by Gibon and Larher (1997) with some modifications. Briefly, 0.1 g of Arabidopsis leaf samples were homogenized in 1 ml of 100 mM HCl for NAD^+ or $NADP^+$ determination or in 1 ml of 100 mM NaOH for NADH or NADPH determination. When testing the plum peel samples, 50 mM HCl and 200 mM NaOH were used. The concentrations of nicotinamide adenine dinucleotide (phosphate) were assayed at 570 nm with a UV-2450 spectrophotometer (Shimadzu) as described by Gibon and Larher (1997).

2.6 | RNA extraction and qRT-PCR analysis

Total RNA was isolated using the sodium dodecyl sulfate-phenol method, according to Malnoy et al. (2001). First-strand cDNA was synthesized using the PrimeScript™ RT reagent Kit (Takara) according to the manufacturer's protocol. Real-time polymerase chain reaction (PCR) was performed with the iQ5 Multicolor Real-Time PCR Detection System (Bio-Rad Laboratories) and SYBR Green Master Mix (SYBR Premix EX TaqTM). *PsActin* and *AtActin* were used to standardize the cDNA samples for the different genes. The primers are listed in Table S2. For each gene assay, three biological replicates were evaluated.

2.7 | RNAi transient assay using the virus-induced gene silencing (VIGS) system

RNAi transient assay was performed as described by Zhai et al. (2016) with some modifications. Briefly, 300–400 bp fragments of the candidate *PsMDH* genes (*PsmMDH*, *PscyMDH*, *PschMDH*) were cloned into pTRV2 to form pTRV2-MDH vectors. The Agrobacterium strain GV3101 containing pTRV1, pTRV2, or pTRV2-MDH independently, and their derivatives were used for the virus-induced gene silencing (VIGS) experiments. The Agrobacterium strain GV3101 containing TRV-VIGS vectors were grown at 28°C in Luria-Bertani medium containing 10 mM 2-morpholinoethanesulfonic acid monohydrate and 20 mM acetosyringone with appropriate antibiotics. After 16 h of incubation, Agrobacterium cells were harvested and re-suspended in the Agrobacterium infiltration buffer (10 mM $MgCl_2$, 10 mM MES, pH 5.6, 150 μM acetosyringone) to a final OD600 of 1.2 (for pTRV1 and pTRV2 and pTRV2-MDH) and shaken for 4–6 h at room temperature before infiltration. A needle (32G Tip ETW) was used to pierce the plum fruits evenly at intervals of 1 cm to a depth of about 0.5 cm. The wounded fruits were submerged into the mixed Agrobacterium strain GV3101 solutions (300 ml) containing equal amounts of pTRV1 and pTRV2 (negative control) or pTRV1 and pTRV2-MDH (treatments) and then vacuumed at the pressure of 0.05 MPa for 0.5 h. The fruits were dried and incubated in the dark for 24 h before light irradiation treatments for 1 week.

2.8 | Statistical analysis

Statistical analysis was carried out using the Statistical Product and Service Solutions software (SPSS; Version 11; IBM). All data were analyzed with *t*-test at $P < 0.05$ and $P < 0.01$.

3 | RESULTS

3.1 | Anthocyanin synthesis and malate metabolism in fruit peel in visible light

The plum fruits at veraison stage were harvested and used for the treatments. Upon exposure to sunlight, both "Red Beauty" and "Early

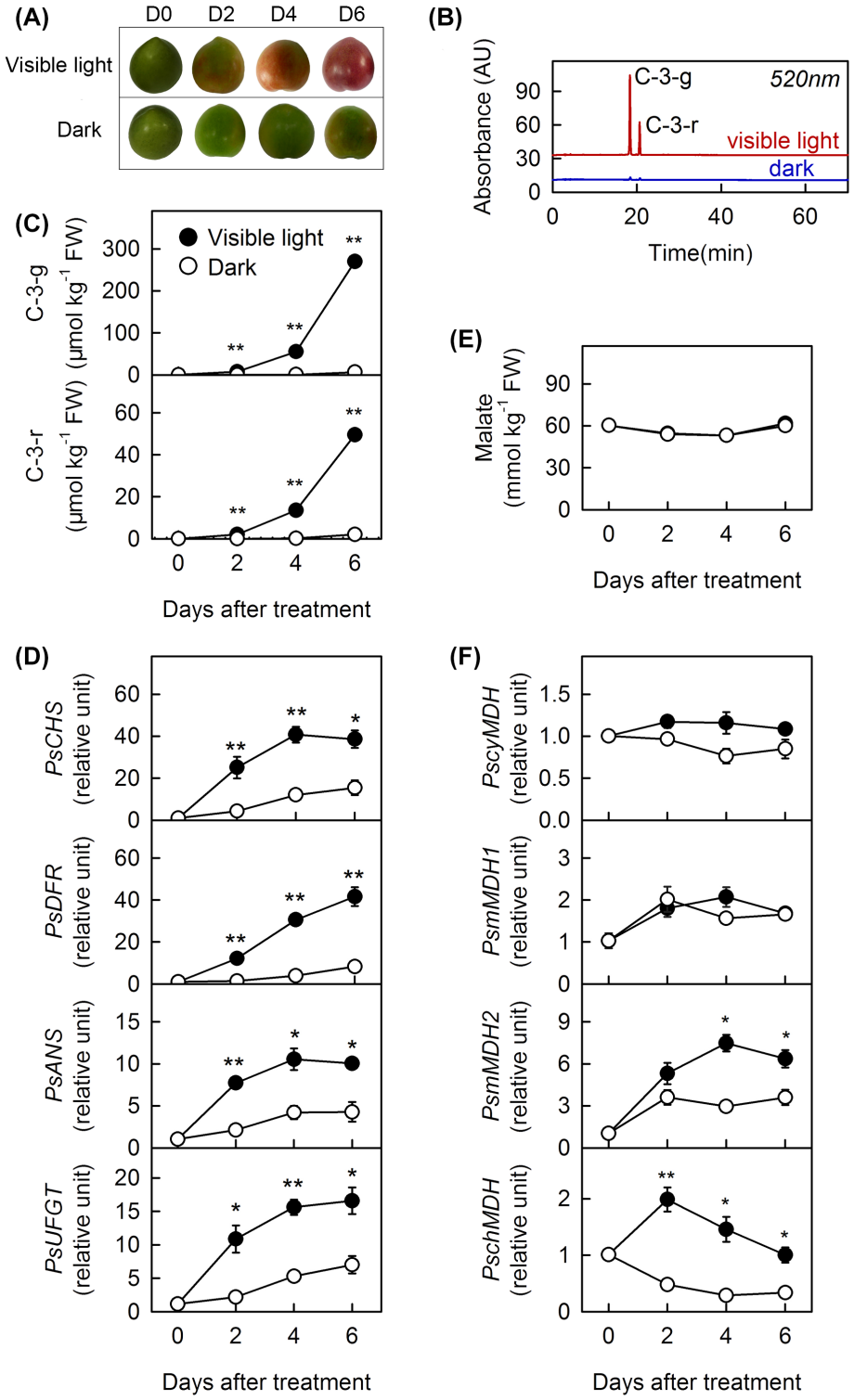

FIGURE 1 Phenotypes (A), chromatograms (B) and contents (C) of anthocyanins, the expression levels of key genes involved in anthocyanin synthesis (D), contents of malate (E) and the expression levels of *PsMDHs* (F) in the peel of "Red Beauty" plum fruits exposed to LED visible light or in the dark. Data are shown as the mean ± SE, $n = 5$ (C, E) or $n = 3$ (D, F). *Significant difference between visible light and dark at $P < 0.05$, **significant difference at $P < 0.01$, *t*-test. *ANS*, anthocyanindin synthase; C-3-g, cyanidin-3-glucoside; C-3-r, cyanidin-3-rutinoside; *chMDH*, chloroplastic malate dehydrogenase; *CHS*, chalcone synthase; *cyMDH*, cytosolic malate dehydrogenase; *DFR*, dihydroflavonol 4-reductase; *mMDH*, mitochondrial malate dehydrogenase; *UFGT*, UDP-glucose: flavonoid 3-*O*-glucosyltransferase

Beauty" plum fruits accumulate abundant anthocyanins in their peels. After filtering out the ultraviolet light, the contents of anthocyanins decreased significantly, but they were still much higher than in fruits kept in the dark (Figure S2), indicating that visible light triggered the anthocyanin synthesis in fruit peels.

To investigate the mechanism of visible light regulation on anthocyanin synthesis, a LED visible light source (Figure S1) was used to irradiate the plum fruits at controlled conditions. Fruits of "Red Beauty" synthesized more anthocyanins in visible light compared to in the dark, with cyanidin-3-glucoside and cyanidin-3-rutinoside being the predominant compounds (Figure 1A–C). After 2 days of irradiation, the contents of anthocyanins were significantly higher than that in the dark, and after 6 days the levels were about 30 times higher in the light than that in the dark. The contents of quercetin-3-glucoside

and quercetin-3-rutinoside also increased faster with the irradiation compared to in the dark (Figure S3). For other phenolic compounds, such as quercetin-3-xyloside, quercetin-3-arabinoside, quercetin-3-rhamnoside, catechin, epicatechin, procyanidin B2, chlorogenic acid, and neochlorogenic acid, the contents hardly changed with the irradiation treatment (Figure S3). The expressions of the key genes involved in anthocyanin synthesis such as *PsCHS*, *PsDFR*, *PsANS*, and *PsUFGT* increased both in the dark and after the visible light irradiation (Figure 1D). However, the levels were significantly higher in visible light than in the dark.

Malate dehydrogenases (MDHs) in plants catalyze the conversion between malate and oxaloacetate, coupling with the conversion between $NAD(P)^+$ and NAD(P)H. In this study, four *MDH*s were cloned from plum and compared with the known *MDH*s in *Arabidopsis thaliana* and Rosaceae plants (Figures S4 and S5). There were two *NAD–MDH*s in mitochondria (*PsmMDH1* and *PsmMDH2*), one *NADP–MDH* in chloroplasts (*PschMDH*), and one *NAD–MDH* in the cytoplasm (*PscyMDH*).

The phylogenetic analysis clearly showed that the *MDH*s of different plant species were roughly divided into three categories. Sequence alignment analysis showed that the similarity of *PschMDH* to *AtchMDH*, *MdchMDH*, *PpechMDH*, and *PmchMDH* was 80%, 92%, 98.8%, and 99.5%, respectively. The similarities of *PsmMDH1*, *PsmMDH2*, or *PscyMDH* to *AtchMDH*, *MdchMDH*, *PpechMDH*, and *PmchMDH* were all less than 40%. The similarity between *PsmMDHs* and *AtmMDH*, *MdmMDH*, *PpemMDH*, or *PmmMDH* was above 80%, while that between *PscyMDH* and the other four *cyMDH*s were also higher than 80%. These results indicate that the sequences of MDHs located at the same organelles were highly conserved among different plants.

During the visible light treatment, the malate content kept unchanged (Figure 1E). The expression of *PscyMDH* hardly changed while that of *PsmMDH1* increased slightly (Figure 1F). However, both genes showed similar levels to those in the dark. The level of *PsMDH2* increased faster with the irradiation treatment. The level of *PschMDH* increased and then decreased in the light, but continuously decreased in the dark, with the value being much higher in the light.

3.2 | Effects of photosynthetic electron transport on anthocyanin synthesis and malate metabolism in fruit peel

The chemical DCMU can inhibit the photosynthetic electron transport (PET) from the reduced primary quinone (electron) acceptor (Q_A^-) to the secondary quinone (electron) acceptor (Q_B), namely, DCMU inhibits the electron transfer from photosystem II (PSII) to photosystem I (PSI). The chemical MV can accept photosynthetic electrons from PSI acceptor side and then inhibit the electron transfer from PSI to $NADP^+$. Both the chemicals may inhibit the production of NADPH and ATP. After treated with the two chemicals, the chlorophyll fluorescence transient and the modulated reflection at 820 nm curves indicate that the PET in fruit peel was well inhibited (Figure S6), consistent with previous studies on leaves (Schansker et al., 2005; Toth et al., 2005). The anthocyanin synthesis and malate metabolism in fruit peel was investigated under the treatment with these two chemicals to explore the relationship between PET and anthocyanin synthesis.

It was found that with the inhibition of PET, the contents of anthocyanins and the expression levels of *PsCHS*, *PsDFR*, *PsANS*, and *PsUFGT* were decreased significantly after 6 days of exposure to visible light (Figure 2A,B). Though the content of malate did not change with DCMU and MV treatments, the expression levels of *PsMDHs* changed after 6 days of visible light exposure (Figure 2C,D). The levels of *PscyMDH* and *PsmMDH1* increased slightly, whereas that of *PsmMDH2* and *PschMDH* decreased significantly. The contents of ATP, NADPH, and NADH decreased, while ADP and $NADP^+$ kept unchanged after DCMU and MV treatments (Figure 2E,F). The content of NAD^+ increased after the treatments.

Upon exposure to visible light, the content of anthocyanins and the levels of the key genes involved in anthocyanin synthesis decreased significantly with the treatment of 1-MCP, while the exogenous application of ethylene significantly increased the anthocyanin contents and the genes expression (Figure 3). These results suggest that the synthesis of anthocyanin in plum peel depends on the ethylene signaling pathway. The combination of DCMU and ethylene treatments enhanced but not inhibited the anthocyanin synthesis, suggesting that the ethylene signaling pathway was downstream compared to the PET, to regulate the anthocyanin synthesis in plum.

3.3 | Effects of *MDH*s silencing/mutation on anthocyanin synthesis in visible light

Using the virus-induced gene silencing (VIGS) system, three *PsMDH*s (*PscyMDH*, *PsmMDH2*, and *PschMDH*) were silenced successfully in the peel of plum fruits (Figure 4A,B). The silencing of *PsMDH*s significantly lowered the contents of anthocyanins (Figure 4C). As for the gene expression, the level of *PsCHS* remained unchanged with the *PsMDH*s silencing treatments. The levels of *PsDFR*, *PsANS*, and *PsUFGT* decreased with the *PsMDH*s silencing treatments, except that *PsDFR* and *PsANS* remained unchanged after silencing *PscyMDH* (Figure 4D).

To further test the relationship between MDHs and anthocyanin synthesis under visible light, wild type of Arabidopsis and its *mdh* (*mmdh1*, *mmdh2*, *chmdh*, *cymdh1*, and *cymdh2*) and *ethylene response1* (*etr1-1*) mutants were used (Figure S7). The plants were treated with visible light at low temperature. It was found that the treatment induced anthocyanin accumulation in the abaxial but not the adaxial side of leaves (Figure 5A and S8). The *mdh* mutants showed significantly lower anthocyanin content, except for the *cymdh1* mutant (Figure 5B). The *etr1-1* mutant also showed significantly lower anthocyanin content compared with the wild type. The expressions of key genes involved in anthocyanin synthesis such as *AtDFR*, *AtLDOX*, and *AtUFGT* exhibited similar patterns to the anthocyanin contents (Figure 5C). The malate contents kept unchanged in the *chmdh*, *cymdh1*, and *cymdh2* mutants, but decreased in the *mmdh1*, *mmdh2*, and *etr1-1* mutants compared

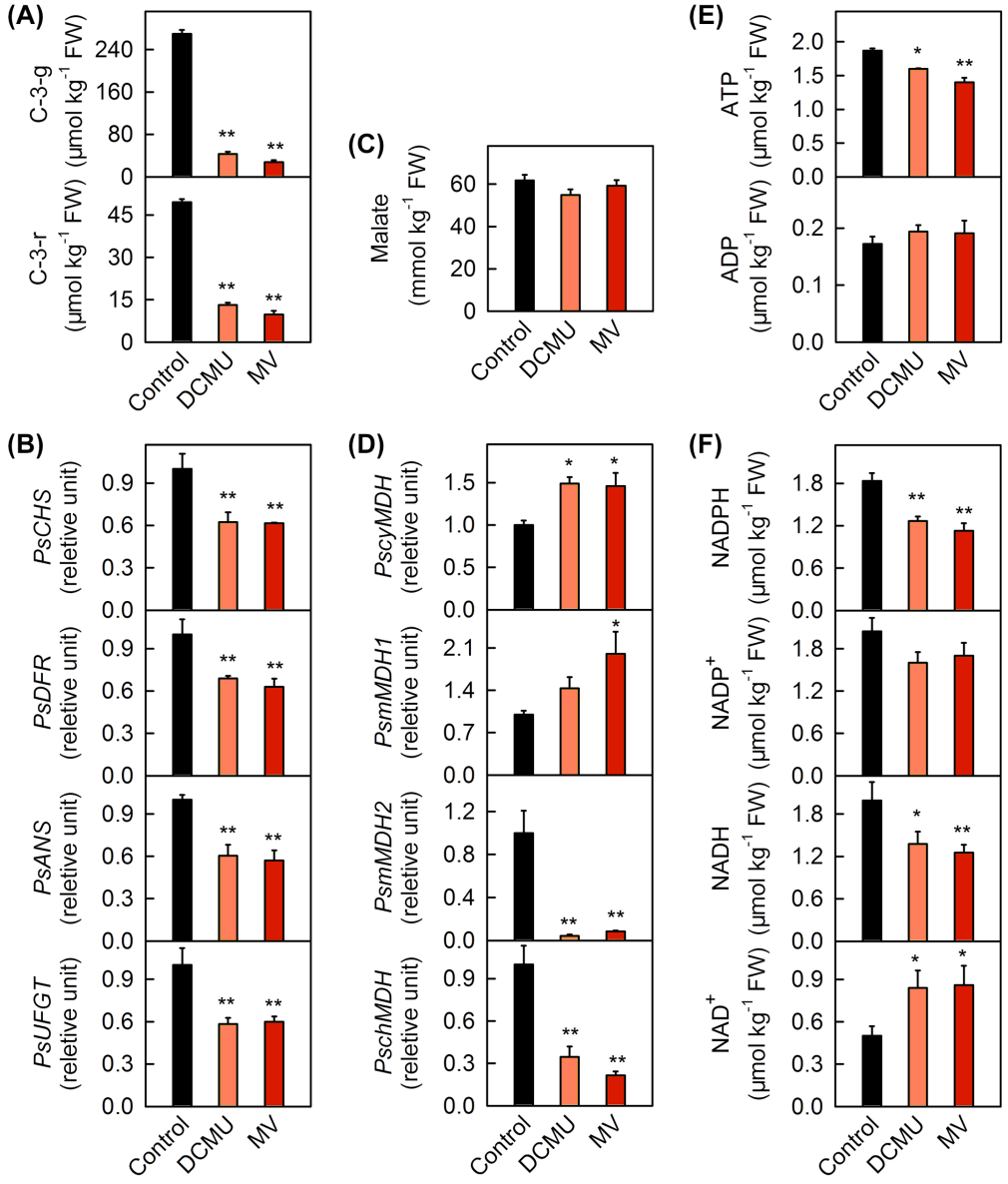

FIGURE 2 Effects of DCMU or MV treatment on the content of anthocyanins (A), the expression levels of key genes involved in anthocyanin synthesis (B), the content of malate (C), the expression levels of *PsMDHs* (D), and the contents of nucleotide (E) and nicotinamide adenine dinucleotide (phosphate) (F) in the peel of "Red Beauty" plum fruits exposed to LED visible light for 6 days. Data are shown as the mean ± SE, $n = 5$ (A, C, E, F) or $n = 3$ (B, D). *, **Significant difference between treatments and control at $P < 0.05$ and $P < 0.01$, *t*-test, respectively. *ANS*, anthocyanindin synthase; C-3-g, cyanidin-3-glucoside; C-3-r, cyanidin-3-rutinoside; *chMDH*, chloroplastic malate dehydrogenase; *CHS*, chalcone synthase; *cyMDH*, cytosolic malate dehydrogenase; DCMU, 3-(3′,4′-dichlorophenyl)-1,1-dimethylurea; *DFR*, dihydroflavonol 4-reductase; *mMDH*, mitochondrial malate dehydrogenase; MV, methyl viologen; *UFGT*, UDP-glucose: flavonoid 3-*O*-glucosyltransferase

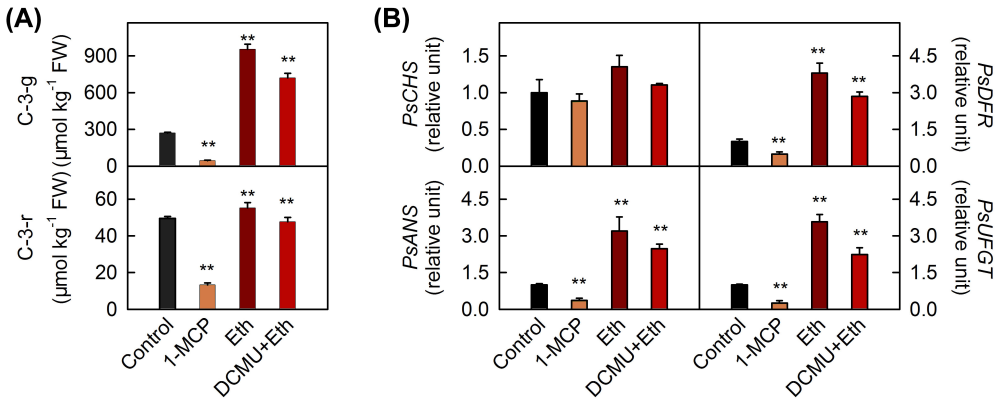

FIGURE 3 Effects of 1-MCP, ethylene (Eth), and the combination of ethylene with DCMU treatments (Eth + DCMU) on the content of anthocyanins (A) and the expression levels of key genes involved in anthocyanin synthesis in the peel of "Red Beauty" plum fruits exposed to LED visible light for 6 days. Data are shown as the mean ± SE, $n = 5$ (A) or $n = 3$ (B). **Significant difference between treatments and control at $P < 0.01$, *t*-test. *ANS*, anthocyanindin synthase; C-3-g, cyanidin-3-glucoside; C-3-r, cyanidin-3-rutinoside; *CHS*, chalcone synthase; *DFR*, dihydroflavonol 4-reductase; *UFGT*, UDP-glucose:flavonoid 3-*O*-glucosyltransferase

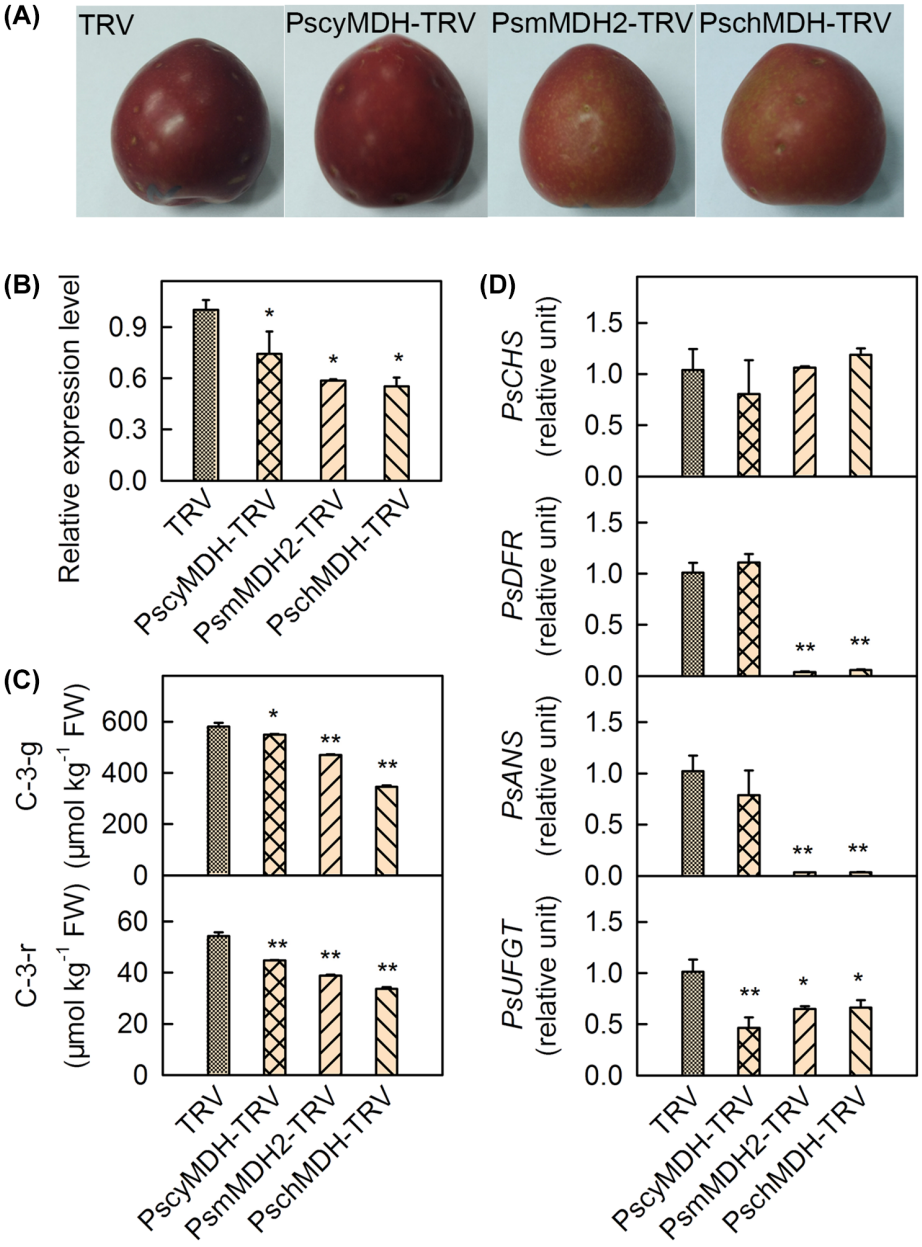

FIGURE 4 Phenotypes (A), *PsMDHs* expressions (B), anthocyanins content (C), and the expression levels of key genes involved in anthocyanin synthesis in the peel of "Red Beauty" plum fruits in visible light after silencing *PsMDHs* through the virus-induced gene silencing (VIGS) system (TRV, fruits treated with empty vector; PscyMDH-TRV, PsmMDH2-TRV, and PschMDH-TRV, fruits with genes silencing). Panel B, the expressions of *PscyMDH*, *PsmMDH2*, and *PschMDH* in the empty vector (TRV) were all set as 1. The genes expression level in the silenced samples (PscyMDH-TRV, PsmMDH2-TRV, and PschMDH-TRV) were compared with their empty vectors, respectively. Data are shown as the mean ± SE (n = 5). *,**Significant difference between gene silencing treatments and control at $P < 0.05$ and $P < 0.01$, t-test, respectively. *ANS*, anthocyanindin synthase; C-3-g, cyanidin-3-glucoside; C-3-r, cyanidin-3-rutinoside; *chMDH*, chloroplastic malate dehydrogenase; *CHS*, chalcone synthase; *cyMDH*, cytosolic malate dehydrogenase; *DFR*, dihydroflavonol 4-reductase; *mMDH*, mitochondrial malate dehydrogenase; *UFGT*, UDP-glucose:flavonoid 3-*O*-glucosyltransferase

with the wild type (Figure 5D). The ATP and ADP contents showed similar patterns to that of malate, except that the content of ATP was lower in *chmdh* mutant, and the content of ADP was lower in *chmdh* and *cymdh2* mutants compared to the wild type (Figure 5E). The contents of NADPH were significantly lower in *mmdh2*, and *chmdh* mutants, whereas the content of $NADP^+$ was also lower in *etr1-1* mutant (Figure 5F). Contents of NADH and NAD^+ were significantly lower in *mmdh1*, *mmdh2*, *chmdh*, and *etr1-1* mutants, but similar in *cymdh1* and *cymdh2* mutants compared with the wild type.

4 | DISCUSSION

The present study clearly demonstrates that both photosynthesis and respiration were involved in the regulation of anthocyanin synthesis in visible light. Moreover, visible light regulated anthocyanin synthesis by controlling the malate metabolism via *MDH*s, and then the ethylene signaling pathway (Figure 6).

Acting on different positions of the PET chain, DCMU and MV can inhibit PET and change the redox state of the plastoquinone (PQ) pool in different ways (Barry et al., 1990; Carstensen et al., 2018; Schansker et al., 2005; Toth et al., 2005). Jeong et al. (2010) proposed that the photosynthetic promotion of anthocyanin synthesis is related to the redox state of PQ pool. In this study, however, as DCMU and MV showed similar effects on anthocyanin synthesis (Figure 2), their inhibitions of the anthocyanin synthesis should not be related to the redox state of the PQ pool. In visible light, the photochemical reaction and PET produce ATP and NADPH to support the Calvin cycle. The inhibition of PET by DCMU and MV lowered the production of ATP and NADPH in plum fruit peel (Figure 2). ATP is the key substrate for

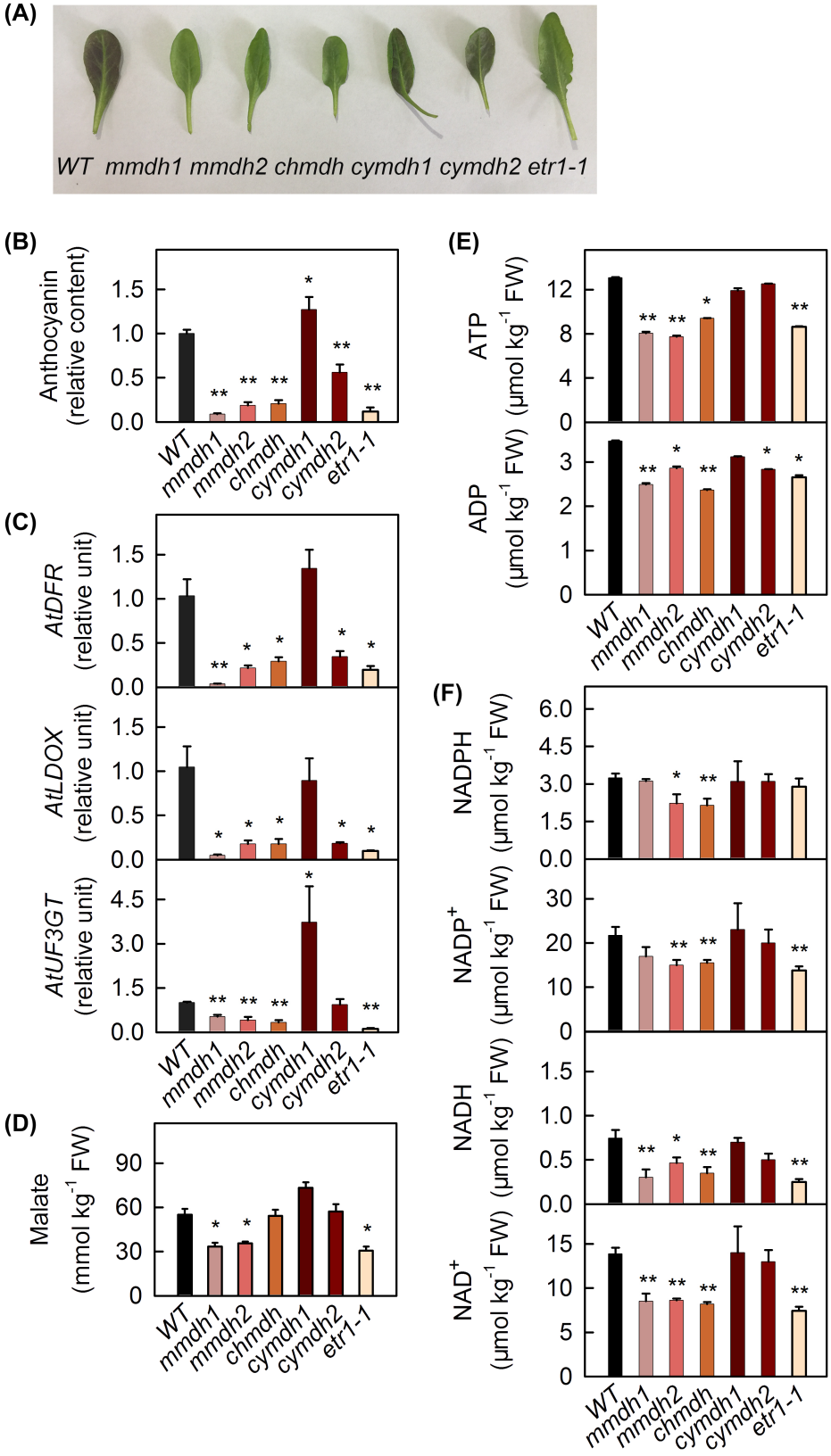

FIGURE 5 Phenotypes (A), anthocyanins content (B), the expression levels of key genes involved in anthocyanin synthesis (C), malate content (D), and the contents of nucleotide (E) and nicotinamide adenine dinucleotide (phosphate) (F) in wild type and different mutants of Arabidopsis exposed to visible light at low temperature. Data are shown as the mean ± SE (n = 5). *,**Significant difference between mutants and wild type at $P < 0.05$ and $P < 0.01$, t-test, respectively. *chmdh*, chloroplastic malate dehydrogenase mutant; *cymdh1*, cytosolic malate dehydrogenase 1 mutant; *cymdh2*, cytosolic malate dehydrogenase 2 mutant; *etr1-1*, ethylene response 1 mutant; *mmdh2*, mitochondrial malate dehydrogenase 2 mutant; WT, wild type (ecotype Colombia 0), *mmdh1*, mitochondrial malate dehydrogenase 1 mutant

ethylene production via the methionine cycle in plants (Yang & Hoffman, 1984). So, the decrease in ATP might result in the down-regulation of anthocyanin synthesis by affecting the production of ethylene in DCMU and MV treated plums (Figure 2). Indeed, it was found that in visible light, the synthesis of anthocyanins in plum fruit peel depended on ethylene signaling (Figure 3).

The primary and secondary metabolites in plum fruits changed greatly during the ripening process (García-Gómez et al., 2020, 2021).

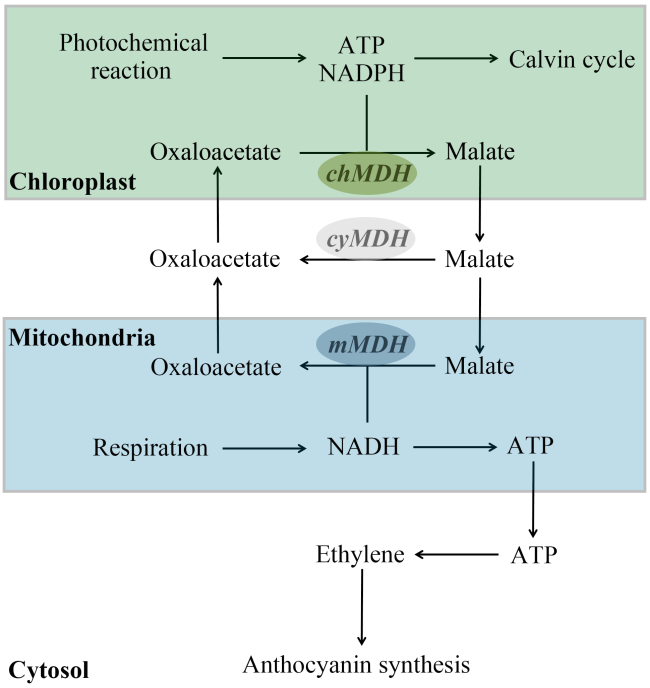

FIGURE 6 The model of regulation of anthocyanin synthesis in plum fruits in visible light. *chmdh*, chloroplastic malate dehydrogenase; *cymdh*, cytosolic malate dehydrogenase; *mmdh*, mitochondrial malate dehydrogenase

The process of fruit ripening is also a process of senescence. During senescence, the capacity of CO_2 fixation decreased faster than that of the photochemical reaction and PET (Biswal & Mohanty, 1978; Hernandez-Gil & Schaedle, 1973). This might result in more ATP and NADPH being accumulated in the chloroplasts of fruit peels. The produced ATP and NADPH could not be directly transported out of the chloroplast (Lim et al., 2020; Winkler & Neuhaus, 1999). However, once the produced NADPH is in excess, chMDH will consume NADPH to produce malate (Lim et al., 2020; Noguchi & Yoshida, 2008). Malate can be transported into the cytoplasm, peroxisomes, and mitochondria by the malate/oxaloacetate shuttles, and then produce NADH catalyzed by MDHs (Li et al., 2020; Raghavendra & Padmasree, 2003; Selinski & Scheibe, 2019; Zhang et al., 2012). In this way, the reducing equivalents produced by photosynthesis could be transported into other organelles. In mitochondria, NADH participates in respiration to produce ATP which could be transported into the cytoplasm (Igamberdiev et al., 1998; Selinski & Scheibe, 2019) to support the metabolisms, for instance, the biosynthesis of ethylene. So, the inhibition of malate transport by the interference of the expressions of *PsMDHs* (*PschMDH*, *PscyMDH*, and *PsmMDH*) might lower the concentration of ATP in the cytoplasm, and as a consequence the ethylene and anthocyanin production (Figures 2 and 4).

Compared with fruit peels, the Rubisco activity and the density of stomata in leaves were much higher (Blanke & Lenz, 1989; Chen & Cheng, 2007; Cheng & Fuchigami, 2000; Simkin et al., 2020). These might result in a higher capacity of photosynthetic CO_2 fixation in leaves compared with fruit peels. However, the photochemical reaction capacity is often comparable between leaves and fruit peels (Brazel & O'Maoileidigh, 2019). The similar producing capacity but much higher consuming capacity of ATP and NADPH in leaves compared with fruit peels means that less ATP and NADPH would be accumulated in the chloroplasts of leaves. It was reported that parts of the ATP in the cytosol were transported into the chloroplasts to support the Calvin cycle in potato leaves (Tjaden et al., 1998). This might explain why at normal conditions, leaves were usually green. However, under chilling stress coupled with light, even at low light conditions, due to the inhibition of the enzymes involved in the Calvin cycle, more accumulation of ATP and NADPH in the chloroplasts might occur (Cai et al., 2018; Kingston-Smith et al., 1997; Zhuang et al., 2020). This may explain why at low temperature, once the malate transport was inhibited in the *mdh* mutants of Arabidopsis, the synthesis of anthocyanin was inhibited (Figure 5). It was interesting to notice that at low temperature, anthocyanins mainly accumulated in the abaxial side of the Arabidopsis leaves (Figure 5 and S8), similar to the results in previous studies (Fiorani et al., 2005). We speculate that this might be due to the relatively lower capacity of the Calvin cycle but similar photochemical reaction in the abaxial side compared with the adaxial side of leaves (Li et al., 2007; Sun et al., 1996; Sun & Nishio, 2001).

In general, visible light regulated the malate transport from the chloroplasts to mitochondria via MDHs. The reducing equivalents transported from chloroplasts into mitochondria controlled the ATP production via respiration. As the substrate of ethylene synthesis, the produced ATP regulated anthocyanin synthesis in visible light. The present study might provide useful information for plum production and breeding.

ACKNOWLEDGMENTS

This work was supported by the National Natural Science Foundation (31171915, 31972366). The authors are grateful to Dr. Hongwei Guo for his donation of the *etr1-1* mutant.

AUTHOR CONTRIBUTIONS

Guojing Zhang, Pengmin Li and Fengwang Ma designed the experiments. Guojing Zhang, Xiaohui Cui and Junping Niu carried out the analysis. Guojing Zhang wrote the manuscript. Pengmin Li revised the manuscript.

DATA AVAILABILITY STATEMENT

The data that support the findings of this study are available from the corresponding author upon reasonable request.

ORCID

Fengwang Ma https://orcid.org/0000-0003-0608-2521
Pengmin Li https://orcid.org/0000-0003-3514-0153

REFERENCES

Ahmad, M. & Cashmore, A.R. (1993) HY4 gene of *A. thaliana* encodes a protein with characteristics of a blue-light photoreceptor. *Nature*, 366, 162–166.

An, J.P., Wang, X.F., Li, Y.Y., Song, L.Q., Zhao, L.L., You, C.X. et al. (2018) EIN3-LIKE1, MYB1, and ETHYLENE RESPONSE FACTOR3 act in a regulatory loop that synergistically modulates ethylene biosynthesis and anthocyanin accumulation. *Plant Physiology*, 178, 808–823.

Barry, P., Young, A.J. & Britton, G. (1990) Photodestruction of pigments in higher plants by herbicide action: I. THE EFFECT OF DCMU (DIURON) ON ISOLATED CHLOROPLASTS. *Journal of Experimental Botany*, 41, 123–129.

Bi, X., Zhang, J., Chen, C., Zhang, D., Li, P. & Ma, F. (2014) Anthocyanin contributes more to hydrogen peroxide scavenging than other phenolics in apple peel. *Food Chemistry*, 152, 205–209.

Biswal, U.C. & Mohanty, P. (1978) Changes in the ability of photophosphorylation and activities of surface-bound adenosine triphosphatase and ribulose diphosphate carboxylase of chloroplasts isolated from the barley leaves senescing in darkness. *Physiologia Plantarum*, 44, 127–133.

Blanke, M.M. & Lenz, F. (1989) Fruit photosynthesis. *Plant, Cell & Environment*, 12, 31–46.

Brazel, A.J. & O'Maoileidigh, D.S. (2019) Photosynthetic activity of reproductive organs. *Journal of Experimental Botany*, 70, 1737–1754.

Brosché, M. & Strid, Å. (2003) Molecular events following perception of ultraviolet-B radiation by plants. *Physiologia Plantarum*, 117, 1–10.

Brown, B.A., Cloix, C., Jiang, G.H., Kaiserli, E., Herzyk, P., Kliebenstein, D.J. et al. (2005) A UV-B-specific signalling component orchestrates plant UV protection. *Proceedings of the National Academy of Sciences of the United States of America*, 102, 18225–18230.

Butler, W.L., Norris, K.H. & Hendricks, H.W.S.B. (1959) Detection, assay, and purification of the pigment controlling photoresponsive development of plants. *Proceedings of the National Academy of Sciences of the United States of America*, 45, 1703–1708.

Cai, B., Li, Q., Liu, F., Bi, H. & Ai, X. (2018) Decreasing fructose-1,6-bisphosphate aldolase activity reduces plant growth and tolerance to chilling stress in tomato seedlings. *Physiologia Plantarum*, 163, 247–258.

Carstensen, A., Herdean, A., Schmidt, S.B., Sharma, A., Spetea, C., Pribil, M. et al. (2018) The impacts of phosphorus deficiency on the photosynthetic electron transport chain. *Plant Physiology*, 177, 271–284.

Chagné, D., Lin-Wang, K., Espley, R.V., Volz, R.K., How, N.M., Rouse, S. et al. (2013) An ancient duplication of apple MYB transcription factors is responsible for novel red fruit-flesh phenotypes. *Plant Physiology*, 161, 225–239.

Chen, L.S. & Cheng, L. (2007) The sun-exposed peel of apple fruit has a higher photosynthetic capacity than the shaded peel. *Functional Plant Biology*, 34, 1038–1048.

Chen, W., Zhang, M., Zhang, G., Li, P. & Ma, F. (2019) Differential regulation of anthocyanin synthesis in apple peel under different sunlight intensities. *International Journal of Molecular Sciences*, 20, 6060.

Cheng, L. & Fuchigami, L.H. (2000) Rubisco activation state decreases with increasing nitrogen content in apple leaves. *Journal of Experimental Botany*, 51, 1687–1694.

Christie, J.M., Arvai, A.S., Baxter, K.J., Heilmann, M., Pratt, A.J., O'Hara, A. et al. (2012) Plant UVR8 photoreceptor senses UV-B by tryptophan-mediated disruption of cross-dimer salt bridges. *Science*, 335, 1492–1496.

El-Kereamy, A., Chervin, C., Roustan, J.P., Cheynier, V., Souquet, J.M., Moutounet, M. et al. (2003) Exogenous ethylene stimulates the long-term expression of genes related to anthocyanin biosynthesis in grape berries. *Physiologia Plantarum*, 119, 175–182.

Espley, R.V., Hellens, R.P., Putterill, J., Stevenson, D.E., Kutty-Amma, S. & Allan, A.C. (2007) Red colouration in apple fruit is due to the activity of the MYB transcription factor, MdMYB10. *The Plant Journal*, 49, 414–427.

Fiorani, F., Umbach, A.L. & Siedow, J.N. (2005) The alternative oxidase of plant mitochondria is involved in the acclimation of shoot growth at low temperature. A study of Arabidopsis AOX1a transgenic plants. *Plant Physiology*, 139, 1795–1805.

García-Gómez, B.E., Ruiz, D., Salazar, J.A., Rubio, M., Martínez-García, P.J. & Martínez-Gómez, P. (2020) Analysis of metabolites and gene expression changes relative to apricot (*Prunus armeniaca* L.) fruit quality during development and ripening. *Frontiers in Plant Science*, 11, 1269.

García-Gómez, B., Salazar, J.A., Nicolás-Almansa, M., Razi, M., Rubio, M., Ruiz, D. et al. (2021) Molecular bases of fruit quality in *Prunus* species: an integrated genomic, rranscriptomic, and metabolic review with a breeding perspective. *International Journal of Molecular Sciences*, 22, 333.

Gibon, Y. & Larher, F. (1997) Cycling assay for nicotinamide adenine dinucleotides: NaCl precipitation and ethanol solubilization of the reduced tetrazolium. *Analytical Biochemistry*, 251, 153–157.

Hernandez-Gil, R. & Schaedle, M. (1973) Functional and structural changes in senescing *Populus deltoides* (Bartr.) chloroplasts. *Physiologia Plantarum*, 51, 245–249.

Hu, D.G., Sun, C.H., Ma, Q.J., You, C.X., Cheng, L. & Hao, Y.J. (2016) MdMYB1 regulates anthocyanin and malate accumulation by directly facilitating their transport into vacuoles in apples. *Plant Physiology*, 170, 1315–1330.

Hu, D.G., Yu, J.Q., Han, P.L., Xie, X.B., Sun, C.H., Zhang, Q.Y. et al. (2019) The regulatory module MdPUB29-MdbHLH3 connects ethylene biosynthesis with fruit quality in apple. *The New Phytologist*, 221, 1966–1982.

Igamberdiev, A., Hurry, V., Kromer, S. & Gardestrom, P. (1998) The role of mitochondrial electron transport during photosynthetic induction. A study with barley (*Hordeum vulgare*) protoplasts incubated with rotenone and oligomycin. *Physiologia Plantarum*, 104, 431–439.

Jeong, S.W., Das, P.K., Jeoung, S.C., Song, J.Y., Lee, H.K., Kim, Y.K. et al. (2010) Ethylene suppression of sugar-induced anthocyanin pigmentation in Arabidopsis. *Plant Physiology*, 154, 1514–1531.

Kim, J.S., Lee, B.H., Kim, S.H., Oh, K.H. & Cho, K.Y. (2006) Responses to environmental and chemical signals for anthocyanin biosynthesis in non-chlorophyllous corn (*Zea mays* L.) leaf. *Journal of Plant Biology*, 49, 16–25.

Kingston-Smith, A.H., Harbinson, J., Williams, J. & Foyer, C.H. (1997) Effect of chilling on carbon assimilation, enzyme activation, and photosynthetic electron transport in the absence of photoinhibition in maize leaves. *Plant Physiology*, 114, 1039–1046.

Lei, M., Zhu, C., Liu, Y., Karthikeyan, A.S., Bressan, R.A., Raghothama, K.G. et al. (2011) Ethylene signalling is involved in regulation of phosphate starvation-induced gene expression and production of acid phosphatases and anthocyanin in Arabidopsis. *The New Phytologist*, 189, 1084–1095.

Li, P.M., Fang, P., Wang, W.B., Gao, H.Y. & Peng, T. (2007) The higher resistance to chilling stress in adaxial side of Rumex K-1 leaves is accompanied with higher photochemical and non-photochemical quenching. *Photosynthetica*, 45, 496–502.

Li, P., Castagnoli, S. & Cheng, L. (2010) Red 'Anjou' pear has a higher photoprotective capacity than green 'Anjou. *Physiologia Plantarum*, 134, 486–498.

Li, Y.Y., Mao, K., Zhao, C., Zhao, X.Y., Zhang, H.L., Shu, H.R. et al. (2012) MdCOP1 ubiquitin E3 ligases interact with MdMYB1 to regulate light-induced anthocyanin biosynthesis and red fruit coloration in apple. *Plant Physiology*, 160, 1011–1022.

Li, P., Ma, F. & Cheng, L. (2013) Primary and secondary metabolism in the sun-exposed peel and the shaded peel of apple fruit. *Physiologia Plantarum*, 148, 9–24.

Li, P., Zhang, Y., Einhorn, T.C. & Cheng, L. (2014) Comparison of phenolic metabolism and primary metabolism between green 'Anjou' pear and its bud mutation, red 'Anjou. *Physiologia Plantarum*, 150, 339–354.

Li, D., Wang, P., Luo, Y., Zhao, M. & Chen, F. (2017) Health benefits of anthocyanins and molecular mechanisms: update from recent decade. *Critical Reviews in Food Science and Nutrition*, 57, 1729–1741.

Li, Y.T., Liu, M.J., Li, Y., Liu, P., Zhao, S.J., Gao, H.Y. et al. (2020) Photoprotection by mitochondrial alternative pathway is enhanced at heat but disabled at chilling. *The Plant Journal*, 104, 403–415.

Lim, S.L., Voon, C.P., Guan, X., Yang, Y., Gardestrom, P. & Lim, B.L. (2020) In planta study of photosynthesis and photorespiration using NADPH

and NADH/NAD(+) fluorescent protein sensors. *Nature Communications*, 11, 1–12.
Lin, C. (2000) Plant blue-light receptors. *Trends in Plant Science*, 5, 337–342.
Liu, Y., Kui, L.W., Espley, R.V., Li, W., Yang, H., Yu, B. et al. (2016) Functional diversification of the potato R2R3 MYB anthocyanin activators AN1, MYBA1, and MYB113 and their interaction with basic helix-loop-helix cofactors. *Journal of Experimental Botany*, 67, 2159–2176.
Maier, A., Schrader, A., Kokkelink, L., Falke, C., Welter, B., Iniesto, E. et al. (2013) Light and the E3 ubiquitin ligase COP1/SPA control the protein stability of the MYB transcription factors PAP1 and PAP2 involved in anthocyanin accumulation in Arabidopsis. *The Plant Journal*, 74, 638–651.
Malnoy, M., Reynoird, J.P., Mourgues, F., Chevreau, E. & Simoneau, P. (2001) A method for isolating total RNA from pear leaves. *Plant Molecular Biology Reporter*, 19, 69–69.
Mano, H., Ogasawara, F., Sato, K., Higo, H. & Minobe, Y. (2007) Isolation of a regulatory gene of anthocyanin biosynthesis in tuberous roots of purple-fleshed sweet potato. *Plant Physiology*, 143, 1252–1268.
Möllering, H. (1974) Malat-bestimmung mit malat-dehydrogenase und glutamat-oxalacetat-transaminase. In: Bergmeyer, H.O. (Ed.) *Methoden der enzymatischen analyse*, Vol. 2. Weinheim: Verlag Chemie, pp. 1636–1639.
Nakabayashi, R., Yonekura-Sakakibara, K., Urano, K., Suzuki, M., Yamada, Y., Nishizawa, T. et al. (2014) Enhancement of oxidative and drought tolerance in Arabidopsis by overaccumulation of antioxidant flavonoids. *The Plant Journal*, 77, 367–379.
Neill, S.O., Gould, K.S., Neill, S.O. & Gould, K.S. (2003) Anthocyanins in leaves: light attenuators or antioxidants? *Functional Plant Biology*, 30, 865–873.
Niu, J., Zhang, G., Zhang, W., Goltsev, V., Sun, S., Wang, J. et al. (2017) Anthocyanin concentration depends on the counterbalance between its synthesis and degradation in plum fruit at high temperature. *Scientific Reports*, 7, 1–16.
Noguchi, K. & Yoshida, K. (2008) Interaction between photosynthesis and respiration in illuminated leaves. *Mitochondrion*, 8, 87–99.
Ponnu, J., Riedel, T., Penner, E., Schrader, A. & Hoecker, U. (2019) Cryptochrome 2 competes with COP1 substrates to repress COP1 ubiquitin ligase activity during Arabidopsis photomorphogenesis. *Proceedings of the National Academy of Sciences of the United States of America*, 116, 27133–27141.
Raghavendra, A.S. & Padmasree, K. (2003) Beneficial interactions of mitochondrial metabolism with photosynthetic carbon assimilation. *Trends in Plant Science*, 8, 546–553.
Schansker, G., Toth, S.Z. & Strasser, R.J. (2005) Methylviologen and dibromothymoquinone treatments of pea leaves reveal the role of photosystem I in the Chl a fluorescence rise OJIP. *Biochimica et Biophysica Acta*, 1706, 250–261.
Schneider, M.J. & Stimson, W.R. (1971) Contributions of photosynthesis and phytochrome to the formation of anthocyanin in turnip seedlings. *Plant Physiology*, 48, 312–315.
Selinski, J. & Scheibe, R. (2019) Malate valves: old shuttles with new perspectives. *Plant Biology*, 21, 21–30.
Shameer, S., Ratcliffe, R.G. & Sweetlove, L.J. (2019) Leaf energy balance requires mitochondrial respiration and export of chloroplast NADPH in the light. *Plant Physiology*, 180, 1947–1961.
Simkin, A.J., Faralli, M., Ramamoorthy, S. & Lawson, T. (2020) Photosynthesis in non-foliar tissues: implications for yield. *The Plant Journal*, 101, 1001–1015.
Smillie, R.M. & Hetherington, S.E. (1999) Photoabatement by anthocyanin shields photosynthetic systems from light stress. *Photosynthetica*, 36, 451–463.
Steyn, W.J., Wand, S.J.E., Holcroft, D.M. & Jacobs, G. (2002) Anthocyanins in vegetative tissues: a proposed unified function in photoprotection. *The New Phytologist*, 155, 349–361.
Sun, J. & Nishio, J. (2001) Why abaxial illumination limits photosynthetic carbon fixation in spinach leaves. *Plant & Cell Physiology*, 1, 1–8.
Sun, J., Nishio, J.N. & Vogelmann, T.C. (1996) High-light effects on CO_2 fixation gradients across leaves. *Plant, Cell & Environment*, 19, 1261–1271.
Tjaden, J., hlmann, T.M., Kampfenkel, K., Henrichs, G. & Neuhaus, H.E. (1998) Altered plastidic ATP/ADP-transporter activity influences potato (*Solanum tuberosum* L.) tuber morphology, yield and composition of tuber starch. *The Plant Journal*, 16, 531–540.
Tohge, T., Zhang, Y., Peterek, S., Matros, A., Rallapalli, G., Tandron, Y.A. et al. (2015) Ectopic expression of snapdragon transcription factors facilitates the identification of genes encoding enzymes of anthocyanin decoration in tomato. *The Plant Journal*, 83, 686–704.
Toth, S.Z., Schansker, G. & Strasser, R.J. (2005) In intact leaves, the maximum fluorescence level (F(M)) is independent of the redox state of the plastoquinone pool: a DCMU-inhibition study. *Biochimica et Biophysica Acta*, 1708, 275–282.
Vincenzo, D.A., Riccardo, A., Giorgia, B., Immacolata, C., Mar, C.M., Ana Beatriz, C.-S. et al. (2014) High *AN1* variability and interaction with basic helix-loop-helix co-factors related to anthocyanin biosynthesis in potato leaves. *The Plant Journal*, 80, 527–540.
Wang, L., Tang, W., Hu, Y., Zhang, Y., Sun, J., Guo, X. et al. (2019) A MYB/-bHLH complex regulates tissue-specific anthocyanin biosynthesis in the inner pericarp of red-centered kiwifruit *Actinidia chinensis* cv. Hongyang. *The Plant Journal*, 99, 359–378.
Winkler, H.H. & Neuhaus, H.E. (1999) Non-mitochondrial ATP transport. *Trends in Biochemical Sciences*, 24, 64–68.
Winslow, R.B. & John, M.C. (2002) Phototropins 1 and 2: versatile plant blue-light receptors. *Trends in Plant Science*, 7, 204–210.
Xiao, J.B. & Hogger, P. (2015) Dietary polyphenols and type 2 diabetes: current insights and future perspectives. *Current Medicinal Chemistry*, 22, 23–38.
Xu, Z.S., Yang, Q.Q., Feng, K. & Xiong, A.S. (2019) Changing carrot color: insertions in DcMYB7 alter the regulation of anthocyanin biosynthesis and modification. *Plant Physiology*, 181, 195–207.
Yang, S.F. & Hoffman, N.E. (1984) Ethylene biosynthesis and its regulation in higher plants. *Annual Review of Plant Physiology*, 35, 155–189.
Yin, R., Arongaus, A.B., Binkert, M. & Ulm, R. (2015) Two distinct domains of the UVR8 photoreceptor interact with COP1 to initiate UV-B signaling in Arabidopsis. *Plant Cell*, 27, 202–213.
Zhai, R., Wang, Z., Zhang, S., Meng, G., Song, L., Wang, Z. et al. (2016) Two MYB transcription factors regulate flavonoid biosynthesis in pear fruit (*Pyrus bretschneideri* Rehd.). *Journal of Experimental Botany*, 67, 1275–1284.
Zhang, L.T., Zhang, Z.S., Gao, H.Y., Meng, X.L., Yang, C., Liu, J.G. et al. (2012) The mitochondrial alternative oxidase pathway protects the photosynthetic apparatus against photodamage in Rumex K-1 leaves. *BMC Plant Biology*, 12, 40.
Zhang, J., Niu, J., Duan, Y., Zhang, M., Liu, J., Li, P. et al. (2015) Photoprotection mechanism in the 'Fuji' apple peel at different levels of photooxidative sunburn. *Physiologia Plantarum*, 154, 54–65.
Zhang, L., Yu, Y., Shi, T., Kou, M., Sun, J., Xu, T. et al. (2020) Genome-wide analysis of expression quantitative trait loci (eQTLs) reveals the regulatory architecture of gene expression variation in the storage roots of sweet potato. *Horticulture Research*, 7, 90.
Zhuang, K., Wang, J., Jiao, B., Chen, C., Zhang, J., Ma, N. et al. (2020) WHIRLY1 maintains leaf photosynthetic capacity in tomato by regulating the expression of RbcS1 under chilling stress. *Journal of Experimental Botany*, 71, 3653–3663.

How to cite this article: Zhang G, Cui X, Niu J, Ma F, Li P. Visible light regulates anthocyanin synthesis via malate dehydrogenases and the ethylene signaling pathway in plum (*Prunus salicina* L.). *Physiologia Plantarum*. 2021;1–11. https://doi.org/10.1111/ppl.13383